Augmenting Adaptive Output Feedback Control of Uncertain Nonlinear Systems with Actuator Nonlinearities

Bong-Jun Yang* , Anthony J. Calise†
School of Aerospace Engineering
Georgia Institute of Technology
Atlanta, Georgia 30332
bong-jun_yang, anthony.calise@ae.gatech.edu

Naira Hovakimyan‡
Department of Aerospace and Ocean Engineering
Virginia Polytechnic Institute and State University
Blacksburg, VA 24061
nhovakimyan@vt.edu

Abstract— **In this paper, we address systematic design of a linear compensator to enhance the performance of an adaptive output feedback control with actuator nonlinearities. The adaptive output feedback controller augments a baseline linear controller. The basic approach involves showing that the augmenting adaptive output feedback architecture is structurally equivalent to a robust internal-loop compensator. The approach addresses a broad class of actuator nonlinearities, and is applicable to non-affine, nonlinear system containing both parametric uncertainty and unmodelled dynamics. We illustrate the main results using a three-disk torsional system, in which the actuator is subject to dead zone and saturation.**

I. Introduction

Actuator nonlinearities have been a major obstacle in guaranteeing stability and performance of adaptive control systems. In this paper, we address how actuator performance can be improved in the adaptive control architecture developed in [1]. From the perspective of adaptive control, actuator nonlinearities can be grouped into two classes: dead zone, backlash, and hysteresis are generally problematic when the control demand is low, and actuator saturation and rate limits degrade performance when the control demand is large.

While actuator nonlinearity is often present, most control design methods either ignore them, or treat a single type of nonlinearity. This is particularly problematic in an adaptive control setting [2]–[4]. Ref. [4] developed an approach called "pseudo-control hedging" (PCH) that is applicable when augmenting a nonlinear, state feedback inverting controller with an adaptive element in the presence of control saturation, and other nonlinear effects. The role of PCH is to protect the adaptive process from attempting to adapt to the effects of actuator nonlinearities. Ref. [5] extends this approach to output feedback, when augmenting a linear controller, and is referred to as "control hedging" (CH). Dead zone, backlash, and hysteresis (and other members of this class) have been mainly addressed by seeking an inverse for a selected nonlinearity [6], [7]. In [8], a neural network (NN) with *jump basis functions* is employed to approximate a dead zone inverse.

A disturbance observer is a servomechanism that estimates and rejects external disturbances so that the system behaves like the plant model. Its use in dealing with actuator nonlinearities is illustrated in [9], for non-adaptive systems, where it is shown that the disturbance observer greatly mitigates the effects that dead zone and backlash have on control system performance. Ref. [10] proposed a robust internal-loop compensator (RIC) and showed its equivalence to a disturbance observer.

In this paper, we show that the control architecture in [1] is equivalent to that of RIC. Using this structural equivalence, We apply the results in [9] to the adaptive control architecture in [1], and incorporate CH from [5] to protect the adaptive process. It is shown that this combination is highly effective for a great variety of actuator nonlinearities (dead zone, backlash, hysteresis and saturation).

The paper is organized as follows: Section II formulates the control problem. In Section III a structural equivalence between a disturbance observer and an augmenting adaptive output feedback architecture is established using the RIC framework. In Section IV we describe the method of augmenting a baseline linear controller with an adaptive element, subjected to nonlinear actuation. The design involves deriving tracking error dynamics and constructing a reduced error observer to generate a teaching signal for an adaptation law. Simulation results with a three-disk pendulum are presented in Section V. Finally, conclusions are given in Section VI.

II. Problem Formulation

For simplicity, the control scheme is presented in a single-input single-output (SISO) setting. Consider an *observable and stabilizable* nonlinear system Σ_p in the following normal form [11, p.541]:

$$\begin{aligned}\dot{\xi} &= A_m\xi + b_m[u+\phi(z_o,\xi,g(u))]\\ \dot{z}_o &= f(z_o,\xi)\\ y &= c_m^T\xi,\end{aligned} \tag{1}$$

where $\xi^T \triangleq [\ x_1 \quad \cdots \quad x_r\ ] \in \mathbb{R}^r$,

$$A_m = \begin{bmatrix} 0 & 1 & 0 & \cdots \\ 0 & 0 & 1 & \cdots \\ \vdots & \vdots & \vdots & \vdots \\ a_1 & a_2 & \cdots & a_r \end{bmatrix}_{r\times r},\ b_m = \begin{bmatrix} 0 \\ 0 \\ \vdots \\ b \end{bmatrix}_{r\times 1},\qquad c_m^T = [\ 1 \quad \ldots \quad 0\ ]_{1\times r}. \tag{2}$$

The vector $z_o \in \mathbb{R}^{n-r}$ contains the states of the internal dynamics, $u \in \mathbb{R}^1$ and $y \in \mathbb{R}^1$ are control and measurement variables, ϕ and f are unknown continuous functions, $\phi(0,0,g(0)) = 0$, $f(0,0) = 0$, and r is the relative degree of y, which is assumed known. The function $g(u)$ represents actuator nonlinearity.

Assumption 1: The internal dynamics $\dot{z}_o = f(z_o,\xi)$ are input-to-state stable [11] with ξ as an input.

A plant model $P_n(s)$, the model used to design a linear controller, is realized by the matrices in (2)

$$\dot{\xi}_m = A_m\xi_m + b_m u_{lc}, \quad y_m = c_m^T\xi_m \tag{3}$$

where $\xi_m \in \mathbb{R}^r$. This implies that the plant model has the relative degree r, and is *fully linearizable* (has no zero dynamics). The

*Graduate Research Assistant, Student Member IEEE, AIAA
†Professor, Senior Member IEEE, Fellow AIAA
‡Associate Professor, Senior Member IEEE

baseline linear controller $C(s)$, designed based on the model in (3), is given by

$$\begin{aligned} \dot{x}_c &= A_c x_c + b_c(y_d - y) \\ u_{lc} &= c_c^T x_c + d_c(y_d - y) \end{aligned} \tag{4}$$

where $x_c \in \mathbb{R}^{n_c}$. Figure 1 represents the typical closed loop system. It is assumed that y_d is bounded, and that for $\Sigma_p = P_n(s)$ ($\phi = 0, f = 0$) all performance specifications are satisfied.

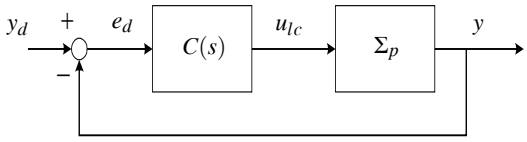

Fig. 1. Typical Feedback Control System

Our control objective is to augment u_{lc} in Figure 1 with an additional control signal u_{ad} so that bounded reference command tracking, i.e. bounded $e_d = y_d - y$, is achieved.

III. Control System Architecture

A. Disturbance Observer $\Longleftrightarrow$ RIC

Figure 2 illustrates how an inner-loop disturbance observer is used to augment the outer-loop controller of Figure 1. Its goal is to force the system Σ_p to behave as the plant model $P_n(s)$ by rejecting external disturbances and modelling errors satisfying a *matching condition*. Its architecture is depicted in Figure 2 for the

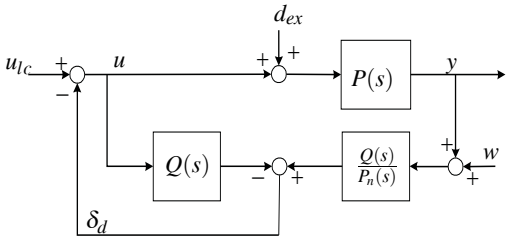

Fig. 2. Disturbance Observer Architecture

case in which the system is linear, $\Sigma_p = P(s)$. The terms d_{ex}, w represent external disturbance and sensor noise, respectively. The Q-filter is designed to reject disturbances below a cut-off frequency [10]. From Figure2, the output y is expressed as

$$y = [P_n(s)u_{lc} + P_n(s)\{1 - Q(s)\}d_{ex} - Q(s)w]\frac{P(s)}{X(s)}, \tag{5}$$

where $X(s) = P_n(s) + [P(s) - P_n(s)]Q(s)$. From (5), we can see that it is desirable that $|1 - Q(j\omega)| \simeq 0$ to reject external disturbances, while $|Q(j\omega)|$ should be small in order to reduce the effect of sensor noise w. Thus, the design of $Q(s)$ is compromise between these conflicting objectives, which can be formulated as a mixed sensitivity optimization problem [12], [13]. A common form for the Q-filter, proposed in [12], is

$$Q(s) = \frac{1 + \sum_{k=1}^{N-r} a_k(\tau s)^k}{1 + \sum_{k=1}^{N} a_k(\tau s)^k}, \tag{6}$$

in which a_k and τ are design parameters. A structural equivalence between the disturbance observer and RIC is established when the Q-filter is selected as

$$Q(s) = \frac{P_n(s)K(s)}{1 + P_n(s)K(s)}, \tag{7}$$

in which $K(s)$ is the compensator designed for the unity feedback system in Figure 1, with $C(s)$ and Σ_p replaced by $K(s)$ and $P_n(s)$, respectively. The relation in (7) implies that if a compensator $K(s)$ is designed for $P_n(s)$ in order to satisfy a given robustness criterion, such as gain/phase margin, the Q-filter is automatically designed.

The feedback control system with RIC as an internal-loop compensator is depicted in Figure 3. The analysis in [10] reveals

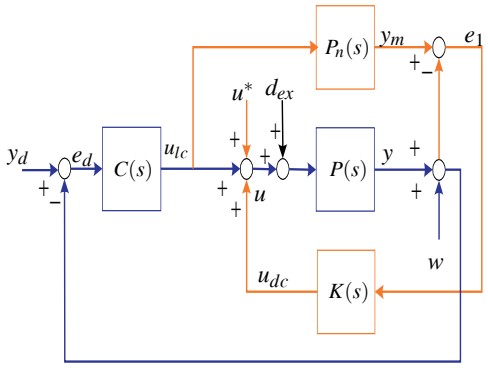

Fig. 3. Robust Internal-loop Compensator (RIC) Architecture

that with $u^* = 0$, the estimated disturbance δ_d in Figure 2 is reformulated as

$$\delta_d = -u_{dc} = -K(s)e_1, \tag{8}$$

in which e_1 is defined by $e_1 = y_m - y$. The control signal u^* is an additional control input used to compensate for plant uncertainty. It can be designed using either a fixed gain method or an adaptive method. From Figure 3 it follows that

$$\begin{aligned} y = &\left[\frac{\{1 + L_n(s)\}P(s)C(s)}{X_c(s)}\right] y_d + \left[\frac{P(s)}{X_c(s)}\right] d_{ex} \\ &- \left[\frac{L(s) + \{1 + L_n(s)\}P(s)C(s)}{X_c(s)}\right] w, \end{aligned} \tag{9}$$

where $L(s) = P(s)K(s)$, $L_n(s) = P_n(s)K(s)$, $X_c(s) = 1 + L(s) + \{1 + L_n(s)\}P(s)C(s)$. With the following definition for d_{eq}

$$d_{eq} \triangleq \left[\frac{P(s)}{P_n(s)} - 1\right] u + \left[\frac{P(s)}{P_n(s)}\right] d_{ex}, \tag{10}$$

which is depicted in Figure 4, we have the transfer function from d_{eq} to y

$$\frac{y(s)}{d_{eq}(s)} = \frac{P_n(s)}{[1 + P_n(s)C(s)][1 + L_n(s)]}. \tag{11}$$

Then, with $w = 0$, the relationship among e_d, y_d and d_{eq} can be

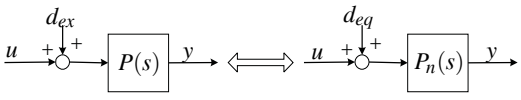

Fig. 4. Reconstruction of the system using equivalent disturbance

expressed as

$$e_d(s) = \frac{1}{1 + P_n(s)C(s)}\left[y_d - \frac{P_n(s)}{1 + L_n(s)}d_{eq}\right]. \tag{12}$$

The effect of d_{eq} on e_d decreases by a factor of $1 + L_n(s)$ compared to the control loop in Figure 1. A stability analysis based on small-gain theorem can be found in [10] for the case of multiplicative model uncertainty, $P(s) = P_n(s)[1 + \Delta(s)]$.

B. Adaptive Output Feedback Control

Figure 5 depicts the adaptive output feedback augmentation architecture developed in [1]. The adaptive controller is designed using the approach in [14]. It is apparent that the architecture

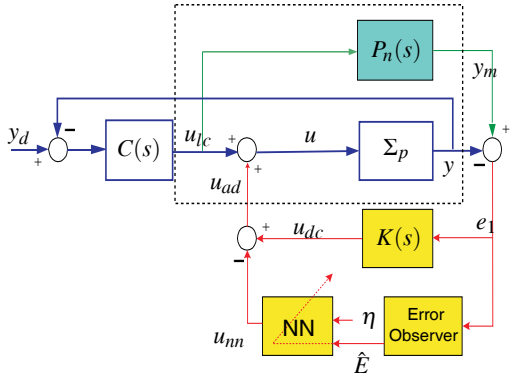

Fig. 5. Adaptive Output Feedback Augmentation Architecture

in Figure 5 is equivalent to the RIC framework in Figure 3 . With $u^* = -u_{nn}$, the architectures are identical if $\Sigma_p = P(s)$. Thus, we can design a linear controller $K(s)$ in Figure 5, using RIC, to achieve performance enhancement when actuator nonlinearities (dead zone, backlash, hysteresis) belong to the class defined in [9]. In addition, input saturation can be treated using the CH method [5] depicted in Figure 6. The term $\hat{g}(u)$ is an estimate for input

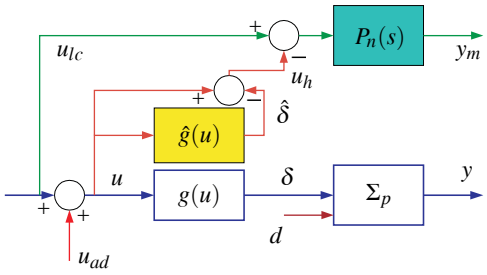

Fig. 6. Implementation of Control Hedging.

saturation. That is, $\hat{g}(u) = \begin{cases} u, & \text{if } |u| \le \hat{u}_{\text{lim}} \\ \text{sgn}(u)\hat{u}_{\text{lim}}, & \text{if } |u| > \hat{u}_{\text{lim}} \end{cases}$, where $\hat{u}_{\text{lim}}$ is an estimate for the control limit u_{lim}. If the control limit is known, $\hat{u}_{\text{lim}} = u_{\text{lim}}$. The rationale of CH combined with the RIC design is as follows. When actuation is nonlinear at low control command levels, the RIC controller boosts the control command. When actuation is nonlinear at high control command levels, CH modifies the control command to $P_n(s)$ to protect the adaptive process.

IV. Adaptive Output Feedback Augmentation

A. Output Tracking Error Dynamics

With CH, the plant model dynamics in (3) are modified as

$$\begin{aligned} \dot{\xi}_m &= A_m\xi_m + b_m(u_{lc} - u_h), \quad u_h = u - \hat{g}(u) \\ y_m &= c_m^T\xi_m, \end{aligned} \tag{13}$$

Define the tracking error vector

$$e = \xi_m - \xi. \tag{14}$$

With the following control signal augmentation

$$u = u_{lc} + u_{ad} = u_{lc} + u_{dc} - u_{nn}, \tag{15}$$

comparing (1) to (13) leads to the following tracking error dynamics

$$\begin{aligned} \dot{e} &= A_m e + b_m(-u_{dc} + u_{nn} - \Phi(z_o, \xi, u)) \\ \dot{z}_o &= f(z_o, \xi) \\ e_1 &= c_m^T e, \end{aligned} \tag{16}$$

where u_{dc} is the control signal designed by RIC, and u_{nn} is an adaptive signal used to approximately cancel the uncertainty $\Phi(z_o, \xi, u)$, which is defined by

$$\Phi(z_o, \xi, u) = \phi(z_o, \xi, u) + (u - \hat{g}(u)). \tag{17}$$

From (15) and (17), it follows that Φ depends on u_{nn} through u, whereas u_{nn} is designed to cancel Φ.

Assumption 2: There exist a fixed point solution for $u_{nn} = \Phi(\cdot, -u_{nn})$ on the domain of interest.

When the actuator is not in saturation, the equation collapses into $u_{nn} = \phi(\cdot, -u_{nn})$. According to the Brouwer fixed point theorem [15], any continuous function with its range contained in a bounded domain must have at least one fixed point. Existence and uniqueness of a fixed point is guaranteed when the mapping $u_{nn} \to \phi$ is a contraction. This can be assured if

$$\left| \frac{\partial \phi}{\partial u} \right| < 1, \tag{18}$$

which is more general than the typical assumption found in the literature [11, p. 603]

$$|\phi(z_o, \xi, u)| \le \rho(z_o, \xi) + k_u|u|, \tag{19}$$

in which a continuous function $\rho(z_o, \xi) \ge 0$ and $k_u \in [0,\ 1)$ are assumed to be known. Also, the condition in (18) is equivalent to the following two conditions [16]:

$$\begin{aligned} &\text{sign}(b) = \text{sign}\left(\frac{\partial \dot{x}_r}{\partial u}\right) \\ &\left| \frac{\partial \dot{x}_r}{\partial u} \right| / 2 < |b| < \infty. \end{aligned} \tag{20}$$

These conditions mean that control reversal is not permitted and there is a lower bound on the estimate of the control effectiveness b of the plant model. When the actuator is in saturation, $\hat{g}(u) = \pm u_{\text{lim}}$. Therefore, Assumption 2 is automatically satisfied unless $\frac{\partial \phi}{\partial u} = 2$. In this case, it is notable that without CH, Assumption 2 is violated [17]. A different viewpoint that uses the mean value theorem to eliminate the fixed point assumption can be found in [18], [19].

A single hidden layer NN is used to approximate Φ in (17). Since the uncertainty Φ is a function of states and control, we recall the result from [20] that enables approximation of unknown bounded processes, using finite input/output history.

Theorem 1: For arbitrary $\varepsilon^* > 0$, there exist bounded constant weights M, N such that:

$$\Phi(z_o, \xi, u) = M^T\sigma(N^T\eta) + \varepsilon(\eta), \ \ \|\varepsilon(\eta)\| \le \varepsilon^*, \tag{21}$$

where $\varepsilon(\eta)$ is the NN reconstruction error and η is the network input vector

$$\begin{aligned} \eta(t) &= [\ 1 \quad \bar{u}_d^T(t) \quad \bar{y}_d^T(t)\ ]^T, \quad \|\eta\| \le \eta^* \\ \bar{u}_d^T(t) &= [u(t) \quad u(t-d) \quad \cdots u(t-(n_1-r-1)d)]^T \\ \bar{y}_d^T(t) &= [y(t) \quad y(t-d) \cdots y(t-(n_1-1)d)]^T \end{aligned} \tag{22}$$

with $n_1 \geq n$ and $d > 0$, σ being a vector of squashing functions $\sigma(\cdot)$, its i^{th} element being defined as $\left[\sigma(N^T\eta)\right]_i = \sigma\left[(N^T\eta)_i\right]$. The adaptive signal u_{nn} is designed as

$$u_{nn} = \widehat{M}^T \sigma(\widehat{N}^T \eta), \tag{23}$$

where $\hat{M}$ and $\hat{N}$ are estimates of M and N to be adapted on-line.

To design $K(s)$ using RIC, a critical step involves defining an equivalent disturbance d_{eq} as in (10). We define it as the approximation error between u_{nn} and Φ in (17)

$$d_{eq} \triangleq -u_{nn} + \Phi(z_o, \xi, u). \tag{24}$$

This implies that the NN approximation error is further attenuated by u_{dc}. The linear controller $K(s)$ is described by

$$\begin{aligned} \dot{x}_{dc} &= A_{dc}x_{dc} + b_{dc}e_1 \\ u_{dc} &= c_{dc}^T x_{dc} + d_{dc}e_1 . \end{aligned} \tag{25}$$

Applying u_{dc} in (25) to (16) leads to the following error dynamics

$$\begin{aligned} \dot{E} &= \bar{A}E - \bar{b}d_{eq} \\ z &= \bar{c}^T E \end{aligned} \tag{26}$$

where $E^T = [\ e^T \quad x_{dc}^T\ ]$, $\bar{c}^T = [\ c_m^T \quad I\ ]$, and

$$\bar{A} = \begin{bmatrix} A_m - b_m d_{dc} c_m^T & -b_m c_{dc}^T \\ b_{dc}c_m^T & A_{dc} \end{bmatrix},\ \bar{b} = \begin{bmatrix} b_m \\ 0 \end{bmatrix}. \tag{27}$$

Since $\bar{A}$ is Hurwitz, for any $Q > 0$, there exists a $P > 0$ such that:

$$\bar{A}^T P + P\bar{A} + Q = 0. \tag{28}$$

Note that the error dynamics in (26) have the same form as in [14], thus the same NN weights update law can be derived.

B. Reduced Error Observer and Adaptation Law

With the definition of d_{eq} in (24), the error dynamics in (16) can be expressed by the following transfer function

$$e_1(s) = P_n(s)[-u_{dc} - d_{eq}]. \tag{29}$$

The term u_{dc} in (8) is an estimate for the equivalent disturbance according to Figure2. Therefore, by the relation between $Q(s)$ and $K(s)$ in (7), Eq.(29) can be rearranged as follows

$$e_1(s) = -P_n(s)(1 - Q(s))d_{eq}. \tag{30}$$

Since the Q-filter is designed so that $(1 - Q(s))d_{eq} \approx 0$ below a cut-off frequency, we construct an error observer assuming $(1 - Q(s))d_{eq} \approx 0$ for the dynamics in (30)

$$\begin{aligned} \dot{\hat{e}} &= A_m\hat{e} + L(e_1 - \hat{e}_1) \\ \hat{e}_1 &= c_m^T\hat{e}. \end{aligned} \tag{31}$$

The observer gain L is designed so that $A_m - Lc_m^T$ is Hurwitz.

Using the estimate in (31), the teaching signal for the NN is constructed as $\widehat{E}^T = [\ \hat{e}^T \quad x_{dc}^T\ ]$. The NN weights $\hat{M}$, $\hat{N}$ are updated according to the following adaptation laws [14]

$$\begin{aligned} \dot{\widehat{M}} &= -\Gamma_M[(\hat{\sigma} - \hat{\sigma}'\widehat{N}^T\eta)\widehat{E}^T P\bar{b} + k\widehat{M}], \\ \dot{\widehat{N}} &= -\Gamma_N[\eta\widehat{E}P\bar{b}\widehat{M}^T\hat{\sigma}' + k\widehat{N}] \end{aligned} \tag{32}$$

in which Γ_M, $\Gamma_N > 0$ are positive definite adaptation gain matrices, $k > 0$ is a $\sigma-$modification constant, $\hat{\sigma} \triangleq \sigma(\hat{N}\eta)$, $\hat{\sigma}'$ is the Jacobian computed at the estimates: $\hat{\sigma}' = \sigma'(\hat{N}\eta)$.

Theorem 2: Consider the system in (1) that satisfies Assumptions 1-2. Together with the NN adaptation rule in (32), the control law in (15) guarantees that the signal e_d is ultimately bounded.

Proof: In [5], [14], it is shown that the adaptive element ensures that the tracking error, e_1, is bounded. Moreover, Assumption 1 ensures that z_o is bounded. Since the linear controller $C(s)$ is designed to stabilize the plant model $P_n(s)$, it immediately follows that if y_d and e_1 are bounded, then e_d is bounded. It is also apparent that when $e_1 = 0$ we recover the tracking performance associated with the existing controller design, with the plant model $P_n(s)$ substituted for the system Σ_p. ■

V. Illustrative Design Example

We demonstrate the approach using a three-disk torsional pendulum in ECP system Inc. [21]. Figure 7 depicts a torsional pendulum system consisting of three disks connected by flexible shafts. The

Fig. 7. The 3-disk Torsional Pendulum System [21].

actuation device, a brushless DC servo motor, apply torque to the bottom disk. The equations of motion for the system are as follows

$$\begin{aligned} J_1\ddot{\theta}_1 + K(\theta_1 - \theta_2) + f_{c_1}(\dot{\theta}_1) &= 0, \\ J_2\ddot{\theta}_2 - K\theta_1 + 2K\theta_2 - K\theta_3 + f_{c_2}(\dot{\theta}_2) &= 0, \\ J_3\ddot{\theta}_3 - K(\theta_2 - \theta_3) + f_{c_3}(\dot{\theta}_3) &= K_{vt}g(u), \end{aligned} \tag{33}$$

where $J_i = 0.103\ \text{kg}\cdot\text{m}^2$, $i = 1,2,3$ are the moments of inertia, $K = 2.2625\ \text{kg}\cdot\text{m}^2/\text{s}^2$ is the spring constant, $K_{vt} = 0.42\ \frac{\text{N}\cdot\text{m}}{\text{V}}$ is the gain from control voltage to torque, and f_{c_i}, $i = 1,2,3$ represents dynamic friction torque, which is described by the model developed in [22]

$$\begin{aligned} &\dot{z}_i = \dot{\theta}_i - \frac{\sigma_f|\dot{\theta}_i|}{G(\dot{\theta}_i)}z_i,\ G(\dot{\theta}_i) = T_c + (T_s - T_c)\exp\left(-(\frac{\dot{\theta}_i}{\dot{\theta}_s})^2\right) \\ &f_{c_i} = \sigma_0 z_i + \sigma_1\dot{z}_i + \sigma_2\dot{\theta}_i,\ i = 1,2,3, \end{aligned} \tag{34}$$

where $T_c = 0.075\ \text{N}\cdot\text{m}$ is the Coulomb friction level, $T_s = 0.083\ \text{N}\cdot\text{m}$ is the stiction torque, and $\dot{\theta}_s = 0.0001$ rad/s is the Stribeck velocity. The constants $\sigma_f = 4\ \text{N}\cdot\text{m}$, $\sigma_0 = 2\ \text{N}\cdot\text{m}$, $\sigma_1 = 0.1\ \text{N}\cdot\text{m}\cdot\text{s}$ are friction parameters, and $\sigma_2 = 0.0018\ \text{kg}\cdot\text{m/s}$ represents a viscous damping coefficient. The control input u is the voltage applied to the control motor, and the stiction value T_c corresponds to the control voltage $0.2V$ with the given gain K_{vt}. The actuator nonlinearity $g(u)$ consists of dead zone and saturation with $u_d = \pm 0.1V$ and $u_{lim} = 1.2V$ as depicted in Figure 8. However, the estimate for the actuator $\hat{g}(u)$ only considers the saturation characteristic. The output is the angular displacement of the bottom disk θ_3, which has relative degree 2. With $f_{c_i} = 0$ and $g(u) = u$, the transfer function from applied voltage to the regulated output is given by

$$\frac{y}{u} = \frac{K_a(s^2 + 2\zeta_{z_1}\omega_{z_1}s + \omega_{z_1}^2)(s^2 + 2\zeta_{z_2}\omega_{z_2}s + \omega_{z_2}^2)}{s(s+c)(s^2 + 2\zeta_{p_1}\omega_{p_1}s + \omega_{p_1}^2)(s^2 + 2\zeta_{p_2}\omega_{p_2}s + \omega_{p_2}^2)}. \tag{35}$$

The parameters are $K_a = 40.46$, $\zeta_{z_1} = 0.009$, $\omega_{z_1} = 9.87$, $\zeta_{z_2} = 0.0035$, $\omega_{z_2} = 25.8$, $c = 0.1786$, $\zeta_{p_1} = 0.00559$, $\omega_{p_1} = 16(\text{rad/sec})$

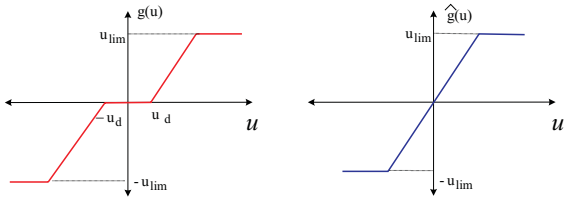

Fig. 8. Actuator Characteristic $g(u)$ and its Estimate $\hat{g}(u)$ in CH.

and $\zeta_{p_2} = 0.00323,\ \omega_{p_2} = 27.7(\text{rad/sec})$. The eigenvalues associated with the zero dynamics are $-0.089 \pm 15.97i$ and $-0.893 \pm 27.66i$. Thus, the internal dynamics are input-to-state stable with y as its input.

The low frequency model without flexible modes is assumed as the plant model

$$\frac{y_m}{u} = \frac{K_n}{s(s+c)}, \tag{36}$$

where $K_n = 13.49, c = 0.18$. Figure 9 compares the frequency response of the plant model in (36) with that in (35). The agreement is quite good at low frequencies but differs significantly at high frequencies due to the unmodelled flexible modes. Comparison of

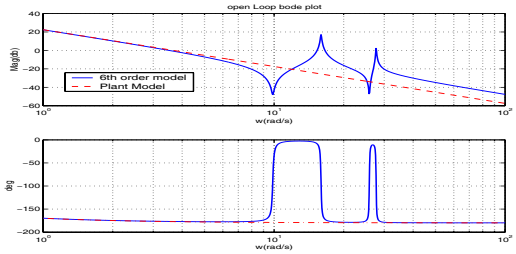

Fig. 9. Open Loop Bode Plots for the 6th Order Model and the Plant Model.

(33) with (36) leads to the following modelling error

$$\Phi = \frac{1}{K_n}[\frac{K}{J_3}(\theta_2 - \theta_3) - \frac{1}{J_3} f_{c_3}(\dot{\theta}_3) + \frac{K_{vt}}{J_3} g(u) + c\dot{\theta}_3 - K_n \hat{g}(u)]. \tag{37}$$

Assumption 2 is assured, since $K_n - K_{vt}/J_3 \neq b$.

The linear controller $C(s)$ is designed as a lead compensator, which results in a dominant mode at $\omega_n = 3rad/s$ and $\zeta = 0.8$ for the nominal system design. This results in $u_{lc} = K_1 \frac{s+b_1}{s+a_1} e_d$, where $K_1 = 0.67, a_1 = 4.8, b_1 = 0.1786$. The RIC controller $K(s)$, which is designed in the same manner as $C(s)$, puts the dominant mode at $\omega = 20rad/s$ and $\zeta = 0.8$. This results in $u_{dc} = 29.65\frac{s+0.18}{s+32} e_1$. From $K(s)$, $Q(s)$ is determined by the relation in (7). Its frequency response is shown together with $1 - Q(s)$ in Figure 10. Figure 10

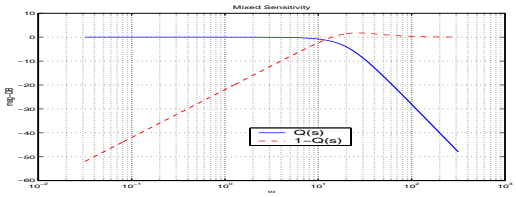

Fig. 10. Frequency Responses of $Q(s)$ and $1 - Q(s)$.

shows that $K(s)$ is designed so that 20db gain decrease is achieved around $\omega = 1$rad/s.

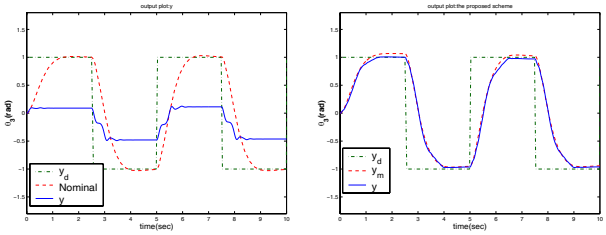

(a) Comparison of the Nominal Loop Response and the Output Regulated only by u_{lc}.

(b) Output Response with the proposed scheme $u = u_{lc} + u_{dc} - u_{nn}$

Fig. 11. Comparison of Output Responses when the System is Regulated Only by u_{lc} and the Proposed Scheme

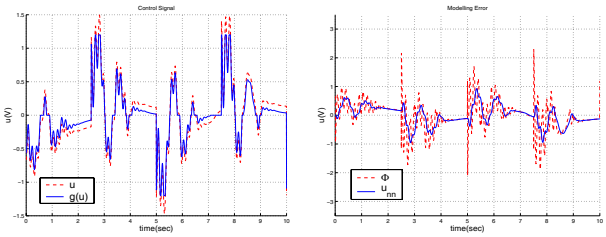

(a) Comparison of u and $g(u)$

(b) Comparison of Φ and u_{nn}

Fig. 12. Control Signals and Actuator Outputs with the Proposed Scheme

The reduced error observer is designed so that the eigenvalues of $A_m - Lc_m^T$ are located at $-82.12 \pm 82.12i$. The SHLNN has 20 neurons in the hidden layer, with its input consisting of 6 delayed values of y and 4 delayed values of u. The network parameters are $\Gamma_M = 0.5I,\ \Gamma_N = 0.5I,\ k = 1.3$.

Figure 11(a) compares output responses of the system in (33) regulated only by the controller $C(s)$ to that of the nominal closed loop system consisting of the plant model in (36) regulated by $C(s)$. The reference command is made up of a square wave of 1 rad. at 0.2 Hz. The response is oscillatory and exhibits a large steady state error. When $C(s)$ is augmented by the elements in Figure 5, the steady steady error and oscillations are drastically decreased as shown in Figure 11(b). The commanded control signal u and the achieved control signal $g(u)$ are compared in Figure 12(a). The modelling error Φ and the adaptive signal u_{nn} are compared in Figure 12(b) to illustrate NN adaptation. The overall compensation scheme is further justified by the results in Figure 13. Without the adaptive signal u_{nn}, as shown in Figure 13(a), the plant model output y_m and the system output y do not converge to each other. Without u_{dc}, Figure 13(b) shows that bounded tracking is achieved, but the response is much more oscillatory than that in Figure 11(b).

The role of CH is illustrated by increasing the magnitude of the reference command to 3 rad. Figure 14 compares the output responses with and without CH. Without CH, the plant model output y_m and the system output y significantly deviate from each other as shown in Figure 14(a). Whenever the actuator is in saturation, the adaptive signal u_{nn} loses track of the uncertainty Φ as shown in Figure 14(c) and 14(e). With CH, almost perfect tracking is maintained with correct NN adaptation as shown in Figure 14(b),14(d) and 14(f).

VI. Conclusions

This paper describes a linear control design to enhance the performance of adaptive augmenting output feedback control when

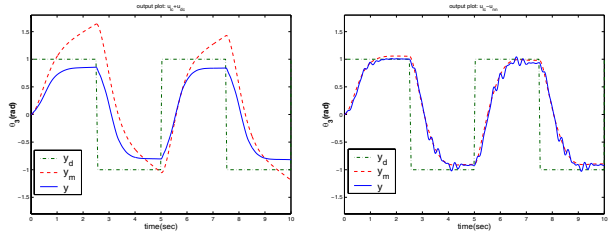

(a) Output Responses with $u = u_{lc} + u_{dc}$

(b) Output Responses with $u = u_{lc} - u_{nn}$

Fig. 13. Output Responses without either u_{dc} or u_{nn}.

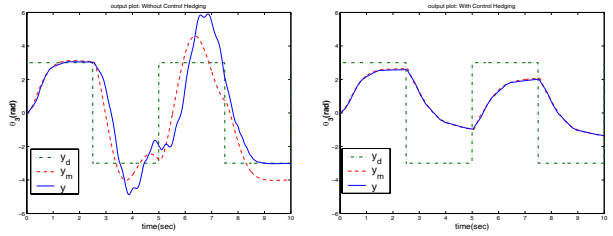

(a) Output Responses Without CH

(b) Output Responses with CH

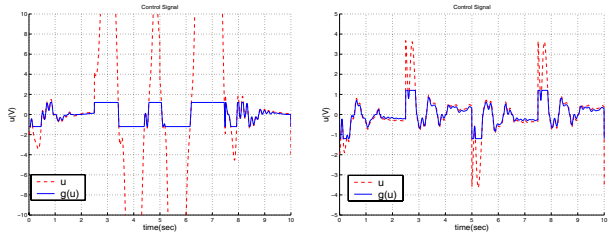

(c) u and $g(u)$ Without CH

(d) u and $g(u)$ With CH

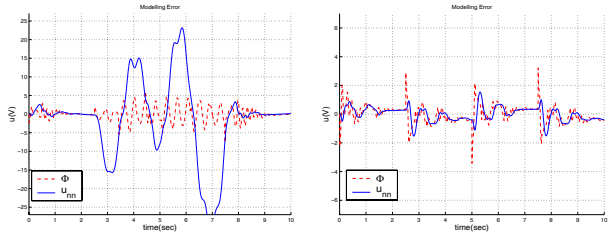

(e) Φ and u_{nn} Without CH

(f) Φ and u_{nn} With CH

Fig. 14. Comparison of responses With and Without CH

a combination of actuator nonlinearities are present. A key ingredient of the linear control design is the structural equivalence between the architecture of augmenting adaptive output feedback control and that of a disturbance observer using the framework of robust internal-loop compensation. Multiple types of actuator nonlinearities can be effectively compensated when the disturbance observer is combined with control hedging. Simulation results illustrate the effectiveness of the approach in control of a three-disk torsional pendulum with dynamic friction, in which the actuator nonlinearities consist of dead zone and saturation.

ACKNOWLEDGEMENT

This research is sponsored by the Air Force Office of Scientific Research, under grant number F4960-01-1-0024.

REFERENCES

[1] A.J. Calise, B.-J. Yang, and J.I. Craig. Augmentation of an existing linear controller with an adaptive element. In *Proceedings of the American Control Conference*, pages 1549–1554, Anchorage,AK, May 2002.

[2] Alexander Leonessa, Wassim M. Haddad, and Tomohisa Hayakawa. Adaptive tracking for nonlinear systems with control constraints. In *Proceedings of the American Control Conference*, Arlington, Virginia, jun 2001.

[3] Marios Polycarpou, Jay Farrell, and Manu Sharma. On-line approximation control of uncertain nonlinear systems: Issues with control input saturation. In *Proceedings of the American Control Conference*, pages 543–548, Denver, CO, June 2003.

[4] Eric N. Johnson and Anthony J. Calise. Limited authority adaptive flight control for reusable launch vehicles. *AIAA Journal of Guidance, Control & Dynamics*, 26(6):906–913, 2003.

[5] A.J. Calise, B.-J. Yang, and J.I. Craig. An augmenting adaptive approach to control of flexible systems. *AIAA Journal of Guidance, Control & Dynamics*, 2004. to appear.

[6] Gang Tao and Petar V. Kokotović. *Adaptive Control of Systems with Actuator and Sensor Nonlinearities*. John Wiley & Sons, Inc., New York, NY, 1996.

[7] Avinash Taware and Gang Tao. *Control of Sandwich Nonlinear Systems*. Springer-Verlag, New York, NY, 2003.

[8] Rastko R. Šelmić and Frank L. Lewis. Deadzone compensation in motion control systems using neural networks. *IEEE Transactions on Automatic Control*, 45(4):602–613, April 2000.

[9] S.M. Shahruz. Performance enhancement of a class of nonlinear systems by disturbance observers. *IEEE/ASME Transactions on Mechatronics*, 5(3):319–323, Sept. 2000.

[10] Bong Keun Kim and Wan Kyun Chung. Performance tuning of robust motion controllers for high-accuracy positioning systems. *IEEE/ASME Tansactions on Mechatronics*, 7(4):500–514, Dec. 2002.

[11] H.K. Khalil. *Nonlinear Systems*. Prentice-Hall, Upper Saddle River, NJ, 1996.

[12] Takaji Umeno, Tomoaki Kaneko, and Yoichi Hori. Robust servosystem design with two degrees of freedom and its application to novel motion control of robot manipulators. *IEEE Transactions on Industrial Electronics*, 40(5):473–485, 1993.

[13] Addisu Tesfaye, Ho Seong Lee, and Masayoshi Tomizuka. A Sensitivity Optimization Approach to Design of a Disturbance Observer in Digital Motion Control Systems. *IEEE Tansactions on Mechatronics*, 5(1):32–38, Mar. 2000.

[14] N. Hovakimyan, F. Nardi, N. Kim, and A.J. Calise. Adaptive output feedback control of uncertain systems using single hidden layer neural networks. *IEEE Transactions on Neural Networks*, 13(6), 2002.

[15] Robert G. Bartle. *The Elements of Real Analysis*. John Wiley & Sons, New York, 2nd edition, 1976.

[16] A.J. Calise, N. Hovakimyan, and M. Idan. Adaptive output feedback control of nonlinear systems using neural networks. *Automatica*, 37(8):1201–1211, 2001.

[17] B.-J. Yang, A.J. Calise, and J.I. Craig. Adaptive output feedback control with input saturation. In *Proceedings of the American Control Conference*, pages 1572–1577, Denver, CO, 2003.

[18] Nakwan Kim. *Improved Methods in Neural Network Based Adaptive Output Feedback Control with Application to Flight Control*. PhD thesis, Georgia Institute of Technology, School of Aerospace Engineering, 2003.

[19] S.S. Ge, C.C. Hang, T.H. Lee, and T. Zhang. *Stable Adaptive Neural Network Control*. Kluwer Academic Publishers, Boston, 2002.

[20] E. Lavretsky, N. Hovakimyan, and A.J. Calise. Upper bounds for approximation of continuous-time dynamics using delayed outputs and feedforward neural networks. *IEEE Transactions on Automatic Control*, 48(9):1606–1610, 2003.

[21] Torsion pendulum appratus, ECP Systems, Inc. `http://www.ecpsystems.com/controls_torplant.htm`.

[22] C. Canudas de Wit, H. Olsson, K.J. Åström, and P. Lischinsky. A new model for control of systems with friction. *IEEE Transactions on Automatic Control*, 40(3):419–425, 1995.